Tetrahedron 65 (2009) 3019–3026

Contents lists available at ScienceDirect

Tetrahedron

journal homepage: www.elsevier.com/locate/tet

Synthesis and in vitro evaluation of botryllazine B analogues as a new class of inhibitor against human aldose reductase

Ryota Saito [a,*], Mai Tokita [a], Keisuke Uda [a], Chikako Ishikawa [b], Mitsutoshi Satoh [b]

[a] Department of Chemistry, Toho University, 2-2-1 Miyama, Funabashi, Chiba 274-8510, Japan
[b] Faculty of Pharmaceutical Sciences, Toho University, 2-2-1 Miyama, Funabashi, Chiba 274-8510, Japan

ARTICLE INFO

Article history:
Received 20 September 2008
Received in revised form 5 January 2009
Accepted 6 January 2009
Available online 14 January 2009

Keywords:
Reductase inhibitor
Pyrazine
Mixed competitive/uncompetitive inhibition

ABSTRACT

Botryllazine B analogues of diverse substitution patterns have been prepared, and their in vitro inhibitory activities against recombinant human aldose reductase (h-ALR2) evaluated. Among the 15 compounds tested, 6-(4-aminophenyl)-2-(4-hydroxyphenyl)carbonylpyrazine (**7b**) proved to be the most potent inhibitor, with IC_{50}=0.91 μM. Kinetic analyses of **7b** and botryllazine B (**1**) revealed that these inhibitors exhibit an unprecedented mixed-type inhibition on h-ALR2 with respect to the substrate D,L-glyceraldehyde, in the presence of NADPH at inhibitor concentrations near the IC_{50} values.

1. Introduction

Aldose reductase (ALR2; EC 1.1.1.21) is an enzyme that catalyzes the transformation of D-glucose into D-sorbitol in the first step of the polyol pathway. Under normal glycemic levels, the metabolic flux of glucose is mostly directed toward the glycolic pathway, and there is little glucose flux through the polyol pathway. However, in people with a condition of diabetes with persistent hyperglycemia, ALR2 activity increases to enhance glucose metabolism through the polyol pathway; as a consequence, the intracellular concentration of sorbitol increases to cause osmotic damage, which leads to chronic complications such as neuropathy, retinopathy, and cataract. Therefore, the inhibition of ALR2 activity has received attention as a useful strategy for attenuating the development of diabetic complications.[1–6]

For decades, numerous organic compounds with diverse structures have been reported as potent ALR2 inhibitors (ARIs). However, most of them have been retreated since undertaking clinical assays, because of unfavorable side effects, low efficacy, or toxicity.[1,7–10] Currently, only epalrestat is available on the market as a drug for treating diabetic neuropathy.[9,10] Thus, the development of new types of organic molecules exhibiting inhibitory activity against ALR2 is highly desirable.

Botryllazine B, a pyrazine alkaloid, was first isolated from the marine ascidian *Botryllus leachi* in 1999 and found to exhibit cytotoxicity against human tumor cell lines.[11] In 2006, De la Fuente et al. reported the inhibitory activity of botryllazine B against human ALR2 (h-ALR2), with an IC_{50} value of 41.4 μM.[12] Although its bioactivity is moderate, botryllazine B has the notable structural feature of lacking glycine or spirohydantoin fragments that are commonly involved in the most highly potent ARIs reported to date.[8–10,13,14] This suggests that this compound could exhibit a novel and unexpected binding mode with the enzyme. Despite this fascinating feature, to the best of our knowledge, no further investigations—such as a structure–activity relationship study on botryllazine B—have been published.

As can be seen from its structure (Fig. 1), botryllazine B has a common fragment, phenymethyl- and phenyl-substituted pyrazine, to coelenteramide, which is derived from luminous marine organisms such as *Aequorea victoria*[15] and *Watasenia scintillans*.[16] With regards this, we have had an interest in the chemistry and utilization of coelenteramide and its derivatives for many years.[17] In a continuing effort to develop useful compounds based on the phenylpyrazine, we have become interested in botryllazine B analogues as ARI candidates. As a first step in this project, we focused our attention to derivatives possessing various phenyl groups that have substituted for the two phenol groups in botryllazine B, because the phenolic hydroxyl groups seem to play important roles in binding to the enzyme through hydrogen bondings. Herein, we report on the synthesis and inhibitory activity of a number of botryllazine B analogues against recombinant h-ALR2, to provide

* Corresponding author.
E-mail address: saito@chem.sci.toho-u.ac.jp (R. Saito).

0040-4020/$ – see front matter © 2009 Elsevier Ltd. All rights reserved.
doi:10.1016/j.tet.2009.01.020

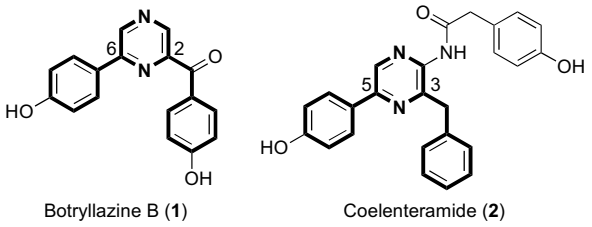

Figure 1. Structures of botryllazine B and coelenteramide.

the first example of structure–activity relationship data among this family of compounds.

2. Results and discussion

Botryllazine B (**1**) and its analogues (**7**–**10**) were synthesized as outlined in Scheme 1.[18] Chloropyrazine (**3**) was converted into 2-tributylstannyl-6-chloropyrazine (**4**). A Stille coupling reaction of **4** with 4-methoxybenzoylchloride afforded chloride **5**, which was then transformed into the botryllazine B analogues **6a**–**i** via a Suzuki–Miyaura coupling reaction with the appropriate phenylboronic acids or a phenylboronic acid pinacol ester. The phenolic methyl ethers for **6a**–**d**,**f**–**i** were cleaved with pyridinium hydrochloride, to afford **1** and **7b**–**d**,**f**–**i** in good yields. 2-Benzoyl-6-(4-hydroxyphenyl)pyrazine, **10**, was synthesized in a reaction sequence similar to that for **6** from **4**, by a Stille coupling with benzoylchloride followed by methyl ether cleavage (Scheme 2). Monoacetate **6j** and diacetate **11** were prepared from **6e** and **1**, respectively, by O-acetylation using standard conditions (acetic anhydride/pyridine), as shown in Scheme 3. An attempt to obtain 6-(4-acetoxyphenyl)-2-(4-hydroxyphenyl)carbonylpyrazine **7j** by methyl ether cleavage of **6j** with boron tribromide was unsuccessful, affording the deacetylation product, **6e** (Scheme 4). The debenzoyl analogue **13** was synthesized via a Suzuki–Miyaura coupling of **3** with 4-methoxyphenylboronic acid, followed by demethylation with pyridinium hydrochloride (Scheme 5). The structures of all synthesized compounds were assigned on the basis of ^{1}H NMR, IR, and mass data, as well as combustion analysis.

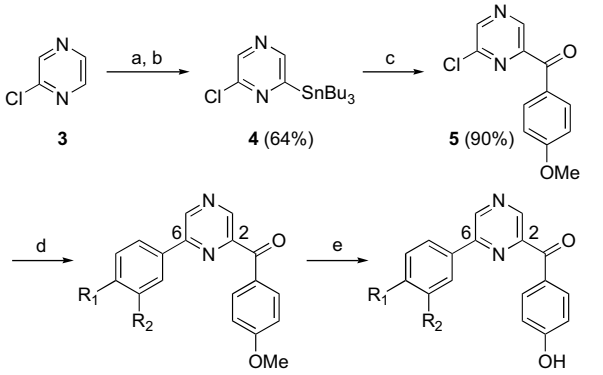

Scheme 1. Reagents and conditions: (a) LiTMP, THF, −75 °C; (b) Bu_3SnCl, THF, −75 °C, 3 h; (c) *p*-$MeOC_6H_4COCl$, $Pd(PPh_3)_4$, toluene, reflux, 3 h; (d) $ArB(OR)_2$, $Pd(PPh_3)_4$, 2 M K_2CO_3, dioxane, reflux, 3–23 h; (e) pyridinium chloride, 200 °C, 40–60 min.

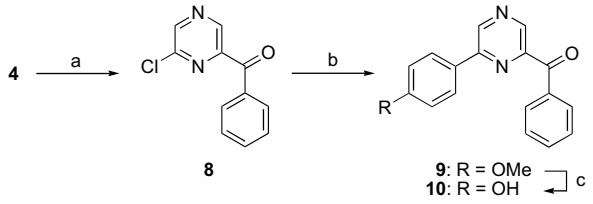

Scheme 2. Reagents and conditions: (a) C_6H_5COCl, $Pd(PPh_3)_4$, toluene, reflux, 16 h, 82%; (b) *p*-$MeOC_6H_4B(OH)_2$, $Pd(PPh_3)_4$, 2 M K_2CO_3, dioxane, reflux, 17 h, 89%; (c) pyridinium chloride, 200 °C, 1 h, 79%.

The ALR2 inhibitory activity of the synthesized botryllazine B (**1**) and its analogues (**6a**–**e**,**j**, **7b**–**d**,**f**–**i**, and **10**–**13**) was evaluated in vitro by measuring their inhibitory effects on the reduction of D,L-glyceraldehyde, using recombinant h-ALR2 in the presence of cofactor NADPH as a reductant.[19] The performed assay was based on the spectrophotometric monitoring of NADPH consumption, which has been proven to be a reliable method.[20] The respective IC_{50} values—which express the 50% inhibition concentration of the compounds on the bioreduction—are shown in Table 1. For comparison, epalrestat and coelenteramide (**2**) were also assayed in the same manner, and those results are also shown.

The IC_{50} value of botryllazine B (**1**) was estimated to be 1.55 μM, representing about 20-fold higher level of activity than the previously reported value (41.4 μM).[12] This difference is probably due to differences in experimental conditions. In the present study, the bioreduction was carried out in a 1-cm quartz cell (total volume, 1.0 mL) at 25 °C, while in the previous evaluation, it was performed in 96-well microtiter plates (total volume, 0.2 mL) at 37 °C. In addition, the enzyme activity in the present assay (1.0–1.2 U/mL) differed from that of the previous one (0.5 mU/mL). In order to verify the accuracy of our experimental results, the IC_{50} value of the epalrestat using the present protocol was estimated and found to be 0.028 μM, which is line with the previously reported value of 0.01–0.026 μM.[21] This finding confirms that the data obtained in this study can be used as absolute values; thus, botryllazine B (**1**) serves as a promising ARI.

An examination of obtained ALR2 inhibitory data reveals several structure–activity trends.

Principally, the compounds bearing the 2-(4-hydroxyphenyl)carbonyl group—namely, **1** and **7**—exhibited considerably enhanced inhibitory activity (IC_{50}=0.91–13.4 μM), compared to the other derivatives. For instance, the methyl ether cleavage in **6**, respectively, affording the corresponding **7**, remarkably improved the activity. The most striking enhancement in the activity was observed with **7c** (IC_{50}=3.03 μM), exhibiting a 50-fold higher inhibitory activity than the corresponding **6c** (IC_{50}=154 μM). Removal of the phenolic hydroxyl group from the C2 phenylcarbonyl group—namely, **10**—also decreased the inhibitory activity. Compound **13**, having no substituent at the C2 position, gave an insignificant bioactivity (IC_{50}=469 μM). These results markedly indicate that the 2-(4-hydroxyphenyl)carbonyl group is essential for gaining effective h-ALR2 inhibitory activity. Coelenteramide (**2**),

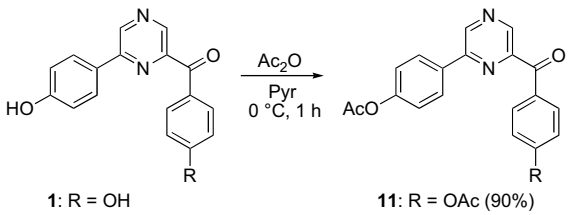

Scheme 3.

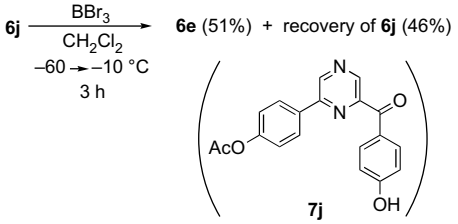

Scheme 4.

the corresponding benzyl analogue, showed lower potency, as expected.

Secondly, among the potent 2-(4-hydroxyphenyl)carbonyl derivatives (**1** and **7**), the compounds possessing hydrogen-bondable substituents on the 6-phenyl (**1**, **7b**, **7h**, and **7i**) showed better inhibitory effects (IC_{50}=0.91–1.78 μM) than the others. The mercapto analogue **7d** was two-fold less active than the corresponding hydroxyl analogue **1** (botryllazine B). Generally, hydrogen bonding between thiol molecules is much weaker than for alcohols, due to the sulfur atom's weaker electronegativity in comparison to oxygen. Compound **7f** having fluorobenzene, which is a commonly used chemotype to replace metabolically unstable phenol group, did not show apparent change in the activity. The dihydroxylated analogue **7i** showed slight improvement in the activity (IC_{50}=1.20 μM), while the *meta* hydroxyl analogue **7h** exhibited a comparable inhibitory activity (IC_{50}=1.78 μM) with the corresponding *para* hydroxy derivative **1**, suggesting that the substitution mode on the 6-phenyl is not essential. From these results, it emerged that a hydrogen-bonding donor/acceptor such as hydroxyl or an amino group on the 6-phenyl is necessary in generating a satisfactory inhibitory effect against the enzyme. In examining the results of **1** and **7b**, the isosteric replacement of the hydroxyl group in **1** with the amino group—which comprises a less efficacious H-bond donor group—led to the most active compound, **7b** (IC_{50}=0.91 μM), among the potent 2-(4-hydroxyphenyl)carbonyl derivatives. The efficacy of **7b** is comparable to that of sorbinil, which is known to be a highly potent ARI (IC_{50}=0.9–20 μM against various ALR2).[10,22] The similar substituent effect on the 6-phenyl was observed even in the less effective methoxy analogues **6**.

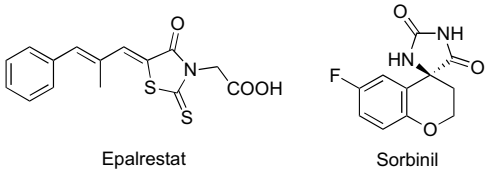

According to the above observations, it appears that an amino group on the 6-phenyl group in combination with 4-hydroxyphenylcarbonyl group at the C2 position is favorable for enhancing the bioactivity. As a consequence, compound **7b** has proved to be a potentially promising ARI, showing an IC_{50} value lower than 1 μM.

Next, in order to survey the inhibition types of **1** and **7b**, the enzyme kinetics for the two compounds were analyzed. The

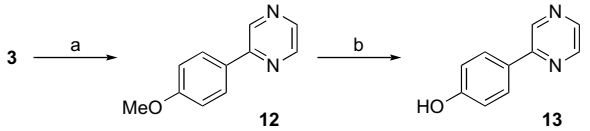

Scheme 5. Reagents and conditions: (a) *p*-$MeOC_6H_4B(OH)_2$, $Pd(PPh_3)_4$, 2 M K_2CO_3, dioxane, reflux, 1.5 h, 94%; (b) pyridinium chloride, 200 °C, 1 h, 88%.

Table 1
In vitro human ALR2 inhibitory activity of botryllazine B derivatives (**1**, **6**, **7**, **10**–**13**), coelenterazine (**2**), and epalrestat

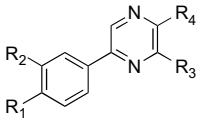

Compd	R_1	R_2	R_3	R_4	IC_{50} (μM)
1	OH	H	COC_6H_4-4-OH	H	1.55
6a	OMe	H	COC_6H_4-4-OMe	H	400
6b	NH_2	H	COC_6H_4-4-OMe	H	49.7
6c	H	H	COC_6H_4-4-OMe	H	154
6d	SH	H	COC_6H_4-4-OMe	H	107
6e	OH	H	COC_6H_4-4-OMe	H	48.8
6j	OAc	H	COC_6H_4-4-OMe	H	81.0
7b	NH_2	H	COC_6H_4-4-OH	H	0.91
7c	H	H	COC_6H_4-4-OH	H	3.03
7d	SH	H	COC_6H_4-4-OH	H	13.4
7f	F	H	COC_6H_4-4-OH	H	2.73
7g	Ph	H	COC_6H_4-4-OH	H	23.3
7h	H	OH	COC_6H_4-4-OH	H	1.78
7i	OH	OH	COC_6H_4-4-OH	H	1.20
10	OH	H	COC_6H_5	H	101
11	OAc	H	COC_6H_4-4-OAc	H	74.9
12	OMe	H	H	H	n.d.[a]
13	OH	H	H	H	469
2	OH	H	COC_6H_5	$NHCOCH_2C_6H_4$-4-OH	51.0
Epalrestat					0.028

[a] No IC_{50} value was determined, owing to its poor solubility toward aqueous solvents.

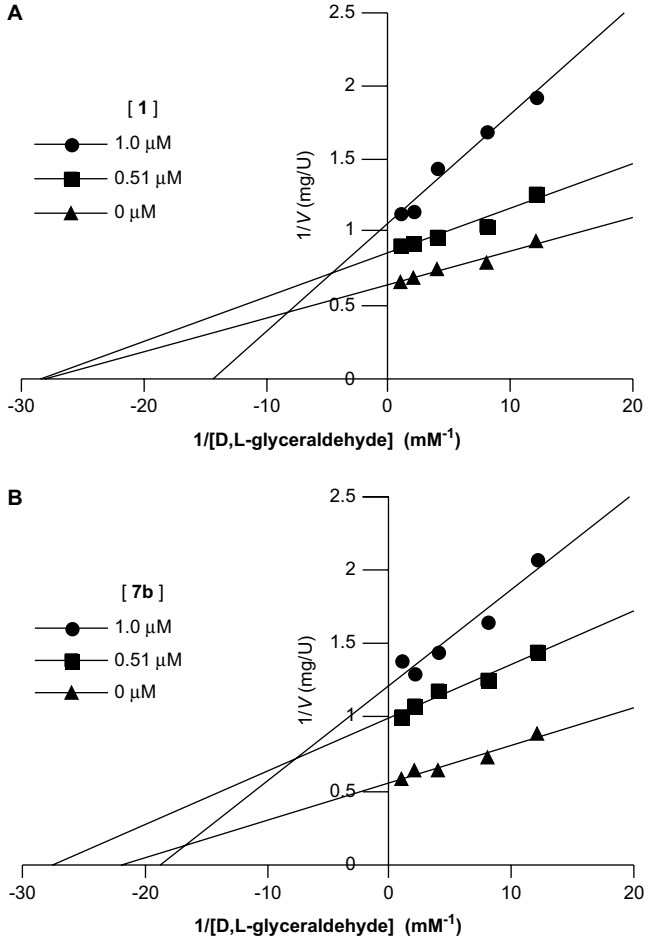

Figure 2. Inhibition of human aldose reductase by **1** (A) and **7b** (B). Double reciprocal plots of the initial enzyme velocities versus concentrations of D,L-glyceraldehyde, in the absence or presence of inhibitors: no inhibitor (closed triangles), 0.51 μM (closed squares), and 1.0 μM (closed circles).

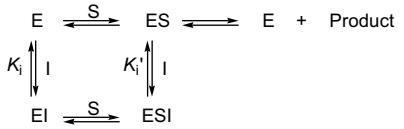

Figure 3. A general model of mixed-type enzyme inhibition. E is the free enzyme, ES is a binary enzyme–substrate complex, EI is the enzyme–inhibitor complex, and ESI is the ternary enzyme–substrate–inhibitor complex.

substrate—D,L-glyceraldehyde at concentrations between 0.08 and 1.0 μM—was reacted with h-ALR2 (3.6 mU/mL) and a test compound at 0, 0.51, and 1.0 μM. Figure 2 shows the double reciprocal plots of the measured initial enzyme velocity versus the concentration of D,L-glyceraldehyde ($1/V$ vs $1/[S]$) in the presence or absence of the test compounds.

In this analysis, compound **1** at 0.51 μM appears to exhibit an uncompetitive inhibition character with respect to the substrate D,L-glyceraldehyde; meanwhile, **7b** at the same concentration displayed a small increase in slope in Figure 2, to show a mixed-type inhibition mode in relation to the substrate. At the higher concentration of the inhibitors (1.0 μM), both **1** and **7b** showed a mixed-type inhibition mode in relation to the substrate.

Figure 3 provides a generalized scheme for the mixed-type inhibition.[23] In this scheme, K_i and K_i' stand for the dissociation constants of the inhibitor from the EI and ESI complexes, respectively. In the presence of an inhibitor, enzyme's Michaelis constant (K_m) and maximum velocity (V_{max}) become the apparent K_m ($K_{m,app}$) and V_{max} ($V_{max,app}$), respectively, as written in Eqs. 1 and 2,[23–25]

$$K_{m,app} = (\alpha/\alpha')K_m \quad (1)$$

$$V_{max,app} = V_{max}/\alpha', \quad (2)$$

where the factors α and α' are defined as Eqs. 3 and 4, respectively.

$$\alpha = 1 + ([I]/K_i) \quad (3)$$

$$\alpha' = 1 + ([I]/K_i') \quad (4)$$

Basically, a mixed-type inhibition is a combination of competitive inhibition and uncompetitive inhibition, and it occurs when the factors α and α' are both greater than unity. The case with $K_i = K_i'$ (i.e., $\alpha = \alpha'$) is called noncompetitive inhibition.[24,25]

To examine the inhibition mechanisms of the potent ARIs in the present study, the apparent kinetic parameters in the presence of the inhibitors (**1** and **7b**) at different concentrations were estimated mathematically using the plotted data in Figure 2. The obtained parameters are listed in Table 2. The experimental Michaelis constant (K_m) for the h-ALR2 with D,L-glyceraldehyde as the substrate in the presence of NADPH was estimated to be 44.4±4.2 μM, by analyzing the double reciprocal plots in the absence of the inhibitors. Using this value, the dissociation constants (or inhibition constants)—K_i and K_i'—for each case were calculated; the data are compiled in Table 2. As can be seen from Table 2, both **1** and **7b** produced the factors α and α', which were larger than unity under the experimental conditions employed; this confirms that these inhibitors produced mixed-type inhibitions on h-ALR2 with respect to the substrate D,L-glyceraldehyde. At the lower concentration (0.51 μM), the K_i values for both **1** and **7b** were larger than the corresponding K_i'. This implies that under this condition, the uncompetitive pathway dominates the others and the inhibitors tend to bind to the enzyme–substrate complex (ES). In contrast, at the higher inhibitor concentration (1.0 μM), the K_i values for both of the inhibitors were lower than the corresponding K_i' values. In this case, the competitive component in the mixed inhibition to afford the EI complex prevailed over the uncompetitive pathway. In other words, at the concentration of 1.0 μM—which approximates to the IC_{50} values—the present inhibitors bind to the free enzyme in such a way that the substrate D,L-glyceraldehyde is prevented from binding to the free enzyme. Previous kinetic studies have demonstrated that the inhibition characteristics of commonly used ARIs—such as sorbinil,[26] tolrestat,[13] zopolrestat,[27] AS-3201,[28] ponalrestat,[29] and epalrestat[21]—in the aldehyde reduction direction have been proved to be uncompetitive; noncompetitive; or mixed ranging from uncompetitive to noncompetitive.[13] To the best of our knowledge, no such profile with a rise in competitive component has been reported save the present observation. Thus, we may say that the newly synthesized **7b**, as well as the naturally occurring **1**, are novel ARIs producing an unprecedented inhibition pattern.

3. Conclusion

We provide here the first example of a structure–activity relationship study on the ALR2 inhibitory activity of botryllazine B and its congeners. Principally, the 4-hydroxyphenylcarbonyl group at the C2 position was found to be essential for good inhibitory effects. In addition, hydrogen-bonding donor substituents such as hydroxyl and an amino group on the 6-phenyl group were found to be important for producing favorable inhibitory effects. Among the tested compound amino derivative **7b** proved to be a promising ARI, exhibiting a submicromolar IC_{50} value (0.91 μM). A kinetic analysis revealed that both **1** and **7b** displayed an unprecedented mixed-type inhibition on h-ALR2, with respect to the substrate D,L-glyceraldehyde at inhibitor concentrations approximating the IC_{50} values.

4. Experimental

4.1. General remarks

All melting points were measured on a MP-21 (Yamato Scientific Co., Ltd., Japan), in open capillary tubes; the values were uncorrected. ^{1}H NMR spectra were recorded on a JNM-ECP400 spectrometer (JEOL Ltd., Japan). Chemical shifts (δ) are reported in parts per million using tetramethylsilane or an undeuteriated solvent as internal standards in the deuterated solvent used. Coupling constants (J) are given in hertz. Infrared (IR) spectra were obtained

Table 2
Effects of inhibitors **1** and **7b** on kinetic parameter of human recombinant aldose reductase in the presence of D,L-glyceraldehyde as the substrate and NADPH as a cofactor at 25 °C. Each value was determined by the least-square approach from double reciprocal plots of three different rate measurements

Inhibitor	$K_{m,app}$ (μM)	$V_{max,app}$ (U/mg)	K_i (μM)	K_i' (μM)	α	α'
1 (0.51 μM)	39.5±2.2	1.20±0.07	2.51±0.48	1.43±0.32	1.2±0.0	1.4±0.1
1 (1.0 μM)	67.3±7.6	1.00±0.07	0.67±0.10	1.53±0.30	2.5±0.2	1.7±0.1
7b (0.51 μM)	33.5±1.0	1.02±0.04	2.34±0.45	0.83±0.09	1.2±0.0	1.6±0.1
7b (1.0 μM)	62.0±9.8	0.84±0.02	0.59±0.13	1.03±0.06	2.8±0.4	2.0±0.1

using FT/IR-4100, FT/IR-460plus, or FT/IR-660plus spectrophotometer (JASCO Co., Ltd., Japan). Fast-atom-bombardment (FAB) mass spectra were taken on a JMS-600-H mass spectrometer (JEOL Ltd., Japan). Xenon was used as a bombardment gas, and all analyses were carried out in positive mode with the ionization energy and the accelerating voltage set at 70 eV and 3 kV, respectively. A mixture of dithiothreitol and α-thioglycerol (1:1 or 1:2) was used as a liquid matrix. Absorption spectra were measured on a UV-240 spectrophotometer (SHIMADZU Co., Ltd., Japan), and combustion analyses were performed on an MT-6 analyzer (Yanaco New Science Inc., Japan). Column chromatography was carried out on silica gel (63–210 μm particle size; Kanto Chemical Co.).

Botryllazine B (**1**) and its synthetic intermediates (**4**, **5**, and **6a**) were prepared according to methods in the literature.[18] Coelenteramide (**2**) was synthesized by a previously reported procedure.[15,30]

All conventional chemicals used in the present study are commercially available, and were used as received. Recombinant h-ALR2 was purchased from Wako Pure Chemical Industries, Ltd. and used without further purification.

4.2. General procedure for Suzuki–Miyaura cross-coupling reactions of chloropyrazines with phenylboronic acid derivatives

Tetrakis(triphenylphosphine)palladium (3 mol %), chloropyrazine (2.8 mmol), and a phenylboronic acid (phenylboronic acid pinacol ester for **6b**) (3.3 mmol) were successively dissolved in 1,4-dioxane (10 mL) under an argon atmosphere. To the solution was added 2 M K_2CO_3 (1.5 mL), and the mixture was refluxed for 5 h. After cooling to room temperature, 25 ml of water was added to the reaction mixture and organic materials were extracted with dichloromethane (40 mL×3). The resulting organic layer was dried over anhydrous magnesium sulfate, and the solvent was evaporated. The obtained residues were purified by column chromatography on silica gel to obtain **6**.

*4.2.1. 6-(4-Aminophenyl)-2-(4-methoxyphenyl)carbonylpyrazine (**6b**)*

Yellow solid (2.84 g, 93%); mp 174 °C (decomp.). ^{1}H NMR (DMSO-d_6, 400 MHz) δ/ppm 9.28 (s, 1H), 8.80 (s, 1H), 8.08 (d, 2H, *J*=8.8 Hz), 7.87 (d, 2H, *J*=8.8 Hz), 7.13 (d, 2H, *J*=8.8 Hz), 6.67 (d, 2H, *J*=8.8 Hz), 5.73 (s, 2H), 3.88 (s, 3H). ^{13}C NMR (DMSO-d_6, 100 MHz) δ/ppm 55.7, 113.9 (×2), 114.0 (×2), 122.0, 128.2, 128.2 (×2), 133.2 (×2), 140.7, 142.4, 149.0, 150.4, 151.3, 163.7, 190.8. IR (KBr) ν_{max}/cm^{-1} 3397, 3318 (νNH), 1637 (νC=O), 1024 (νC–O). FABMS (DTT/TG=1:2) *m*/*z* 306 [M+H]$^+$. Anal. Calcd for $C_{18}H_{13}N_3O_2\cdot 0.1H_2O$: C, 70.39; H, 4.96; N, 13.68. Found: C, 70.41; H, 5.00; N, 13.50.

*4.2.2. 2-(4-Methoxyphenyl)carbonyl-6-phenylpyrazine (**6c**)*

Colorless solid (368 mg, 92%); mp 114–115 °C. ^{1}H NMR ($CDCl_3$, 400 MHz) δ/ppm 9.21 (s, 1H), 9.13 (s, 1H), 8.25 (d, 2H, *J*=8.8 Hz), 8.08 (dd, 2H, *J*=7.9 and 2.2 Hz), 7.51–7.56 (m, 3H), 7.02 (d, 2H, *J*=8.8 Hz), 3.92 (s, 3H). ^{13}C NMR ($CDCl_3$, 100 MHz) δ/ppm 55.7, 113.8 (×2), 127.2 (×2), 128.7, 129.3 (×2), 130.5, 133.8 (×2), 135.7, 143.5, 143.9, 149.8, 150.5, 164.1, 190.7. IR (KBr) ν_{max}/cm^{-1} 1657 (νC=O), 1026 (νC–O). FABMS (DTT/TG=1:2) *m*/*z* 291 [M+H]$^+$. Anal. Calcd for $C_{18}H_{14}N_2O_2$: C, 74.47; H, 4.86; N, 9.65. Found: C, 74.73; H, 4.91; N, 9.53.

*4.2.3. 6-(4-Mercaptophenyl)-2-(4-methoxyphenyl)-carbonylpyrazine (**6d**)*

Pale yellow solid (140 mg, 43%); mp 101–102 °C. ^{1}H NMR ($CDCl_3$, 400 MHz) δ/ppm 8.88 (s, 1H), 8.41 (s, 1H), 8.03 (d, 2H, *J*=8.8 Hz), 7.66 (dd, 2H, *J*=7.3 and 1.9 Hz), 7.46–7.52 (m, 3H), 6.84 (d, 2H, *J*=8.8 Hz), 3.89 (s, 3H). ^{13}C NMR (DMSO-d_6, 100 MHz) δ/ppm 55.6, 113.7 (×2), 127.6, 128.0, 129.8, 130.0 (×2), 133.2 (×2), 135.1 (×2), 141.0, 144.6, 149.2, 155.4, 163.5, 188.9. IR (KBr) ν_{max}/cm^{-1} 1647 (νC=O), 1024 (νC–O). MS (FAB$^+$, DTT/TG=1:2) *m*/*z* 323 [M+H]$^+$. Anal. Calcd for $C_{18}H_{14}N_2O_2S$: C, 67.06; H, 4.38; N, 8.69. Found: C, 67.34; H, 4.46; N, 8.49.

*4.2.4. 6-(4-Hydroxyphenyl)-2-(4-methoxyphenyl)carbonylpyrazine (**6e**)*

The reaction of **5** with (4-*tert*-butyldimethylsilyloxyphenyl)-boronic acid afforded the deprotected compound **6e** directly as an yellow solid (198 mg, 63%); mp 182 °C (decomp.). ^{1}H NMR ($CDCl_3$, 400 MHz) δ/ppm 9.14 (s, 1H), 9.05 (s, 1H), 8.22 (d, 2H, *J*=8.8 Hz), 8.00 (d, 2H, *J*=8.8 Hz), 7.01 (d, 2H, *J*=8.8 Hz), 6.98 (d, 2H, *J*=8.8 Hz), 5.28 (s, 1H), 3.92 (s, 3H). ^{13}C NMR (DMSO-d_6, 100 MHz) δ/ppm 55.7, 114.0 (×2), 116.1 (×2), 126.0, 128.1, 128.7 (×2), 133.3 (×2), 141.9, 143.1, 149.1, 149.9, 159.8, 163.7, 190.7. IR (KBr) ν_{max}/cm^{-1} 3323 (νOH), 1638 (νC=O), 1164, 1012 (νC–O). FABMS (DTT/TG=1:2) *m*/*z* 307 [M+H]$^+$. Anal. Calcd for $C_{18}H_{14}N_2O_3$: C, 70.58; H, 4.61; N, 9.15. Found: C, 70.51; H, 4.71; N, 9.00.

*4.2.5. 6-(4-Fluorophenyl)-2-(4-methoxyphenyl)carbonylpyrazine (**6f**)*

Colorless solid (210 mg, 84%); mp 139–140 °C. ^{1}H NMR ($CDCl_3$, 400 MHz) δ/ppm 9.17 (s, 1H), 9.10 (s, 1H), 8.21 (d, 2H, *J*=8.8 Hz), 8.07 (dd, 2H, *J*=8.4 and 5.5 Hz), 7.21 (t, 2H, *J*=8.4 Hz), 7.01 (d, 1H, *J*=8.8 Hz), 3.92 (s, 3H). ^{13}C NMR ($CDCl_3$, 100 MHz) δ/ppm 56.0, 114.1 (×2), 116.6, 116.9, 128.9, 129.4, 129.5, 132.2, 134.0 (×2), 143.4, 144.1, 149.9, 150.1, 163.5, 164.5, 190.9. IR (KBr) ν_{max}/cm^{-1} 1655 (νC=O), 1235 (νC–F), 1014 (νC–O). FABMS (DTT/TG=1:2) *m*/*z* 309 [M+H]$^+$. Anal. Calcd for $C_{18}H_{13}FN_2O_2\cdot 0.1$hexane: C, 70.42; H, 4.48; N, 8.83. Found: C, 70.58; H, 4.34; N, 8.70.

*4.2.6. 6-(4-Biphenylyl)-2-(4-methoxyphenyl)carbonylpyrazine (**6g**)*

Colorless solid (271 mg, 90%); mp 135–136 °C. ^{1}H NMR (DMSO-d_6, 400 MHz) δ/ppm 9.56 (s, 1H), 9.06 (s, 1H), 8.27 (d, 2H, *J*=8.4 Hz), 8.12 (d, 2H, *J*=8.8 Hz), 7.88 (d, 2H, *J*=8.8 Hz), 7.77 (d, 2H, *J*=7.7 Hz), 7.51 (t, 2H, *J*=7.7 Hz), 7.42 (t, 1H, *J*=7.7 Hz), 7.15 (d, 2H, *J*=8.8 Hz), 3.90 (s, 3H). ^{13}C NMR (DMSO-d_6, 100 MHz) δ/ppm 55.7, 114.0 (×2), 126.8 (×2), 127.4 (×3), 127.6 (×2), 128.0, 129.1 (×2), 133.3 (×2), 134.2, 139.2, 141.9, 143.2, 143.9, 149.2, 149.3, 163.8, 190.5. IR (KBr) ν_{max}/cm^{-1} 1651 (νC=O), 1020 (νC–O). FABMS (DTT/TG=1:2) *m*/*z* 367 [M+H]$^+$. Anal. Calcd for $C_{24}H_{18}N_2O_2$: C, 78.67; H, 4.95; N, 7.65. Found: C, 78.95; H, 5.04; N, 7.56.

*4.2.7. 6-(3-Hydroxyphenyl)-2-(4-methoxyphenyl)carbonylpyrazine (**6h**)*

Pale yellow solid (212 mg, 86%); mp 152–153 °C. ^{1}H NMR (DMSO-d_6, 400 MHz) δ/ppm 9.76 (s, 1H), 9.42 (s, 1H), 9.02 (s, 1H), 8.09 (d, 2H, *J*=8.8 Hz), 7.61 (d, 1H, *J*=7.7 Hz), 7.54 (s, 1H), 7.36 (t, 1H, *J*=7.7 Hz), 7.14 (d, 2H, *J*=8.8 Hz), 6.93 (d, 1H, *J*=7.7 Hz), 3.89 (s, 3H). ^{13}C NMR (DMSO-d_6, 100 MHz) δ/ppm 55.7, 113.6, 114.0 (×2), 117.5, 117.8, 128.0, 130.3, 133.3 (×2), 136.5, 143.2, 143.8, 149.2, 149.6, 158.1, 163.7, 190.5. IR (KBr) ν_{max}/cm^{-1} 3306 (νOH), 1652 (νC=O), 1161, 1016 (νC–O). FABMS (DTT/TG=1:2) *m*/*z* 307 [M+H]$^+$. Anal. Calcd for $C_{18}H_{14}N_2O_3\cdot 0.1$hexane: C, 70.86; H, 4.83; N, 8.89. Found: C, 70.86; H, 4.66; N, 8.69.

*4.2.8. 6-(3,4-Dimethoxyphenyl)-2-(4-methoxyphenyl)-carbonylpyrazine (**6i**)*

Pale yellow solid (278 mg, 98%); mp 127–128 °C. ^{1}H NMR ($CDCl_3$, 400 MHz) δ/ppm 9.17 (s, 1H), 9.06 (s, 1H), 8.26 (d, 2H, *J*=8.8 Hz), 7.65–7.69 (m, 2H), 7.01 (d, 1H, *J*=8.4 Hz), 7.00 (d, 2H, *J*=8.8 Hz), 3.97 (s, 3H), 3.96 (s, 3H), 3.91 (s, 3H). ^{13}C NMR ($CDCl_3$, 100 MHz) δ/ppm 55.7, 56.1, 56.2, 109.9, 111.5, 113.7 (×2), 120.0, 128.5, 128.8, 133.8 (×2), 142.9, 143.1, 149.5, 149.8, 150.2, 151.3, 164.1, 190.7. IR (KBr) ν_{max}/cm^{-1} 1653 (νC=O), 1026 (νC–O). FABMS (DTT/TG=1:2) *m*/*z* 351 [M+H]$^+$. Anal. Calcd for $C_{20}H_{18}N_2O_4$: C, 68.56; H, 5.18; N, 8.00. Found: C, 68.40; H, 5.16; N, 7.83.

4.3. Synthesis of 6-(4-acetoxyphenyl)-2-(4-methoxyphenyl)carbonylpyrazine (6j)

To a solution of **6e** (201 mg, 656 μmol) in pyridine (1.0 mL) was added acetic anhydride (0.20 mL, 2.1 mmol) at 0 °C, under an argon atmosphere. The mixture was then stirred at the same temperature for 1 h. The reaction was terminated with the addition of water (30 mL), and the organic materials were extracted with ethyl acetate (30 mL×3). The combined organic layer was washed once with 5% citric acid (30 mL) and then dried over anhydrous magnesium sulfate. After evaporating the solvent, the resulting materials were purified by recrystallization from ethyl acetate, to afford **6j** as a colorless solid (135 mg). The filtrate of the recrystallization was concentrated and further purified by column chromatography on silica gel to obtain **6j** as colorless solids (84.2 mg). The total yield of **6j** was 219.2 mg (96%); mp 129–130 °C. ^{1}H NMR ($CDCl_3$, 400 MHz) δ/ppm 9.19 (s, 1H), 9.12 (s, 1H), 8.22 (d, 2H, J=9.2 Hz), 8.11 (d, 2H, J=8.8 Hz), 7.26 (d, 2H, J=8.8 Hz), 7.01 (d, 2H, J=9.2 Hz), 3.92 (s, 3H), 2.35 (s, 3H). ^{13}C NMR (DMSO-d_6, 100 MHz) δ/ppm 21.0, 55.8, 114.1 (×2), 122.8 (×2), 128.0, 128.5 (×2), 132.9, 133.4 (×2), 143.3, 143.9, 149.0, 149.3, 152.3, 163.9, 169.2, 190.6. IR (KBr) ν_{max}/cm^{-1} 1743, 1659 (νC=O), 1161, 1014 (νC–O). FABMS (DTT/TG=1:2) m/z 349 [M+H]$^+$. Anal. Calcd for $C_{20}H_{16}N_2O_4$: C, 68.96; H, 4.63; N, 8.04. Found: C, 66.80; H, 4.63; N, 7.34.

4.4. Reaction of 6j with boron tribromide

To a solution of **6j** (112 mg, 0.32 mmol) in dichloromethane (40 mL) was added 1.0 mL of 1.0 M solution of boron tribromide in dichloromethane at −60 °C under argon atmosphere. The mixture was then stirred under argon for 3 h, during which the temperature was allowed to rise to −10 °C. The reaction was quenched by adding 5 mL of methanol to the reaction mixture at −30 °C. After removal of the solvents, the resulting materials were dissolved in water (40 mL) and neutralized with saturated sodium hydrogen carbonate. Organic materials were extracted with ether (40 mL×3), and the combined organic layer was dried over anhydrous magnesium sulfate. After evaporation of the solvent, the crude product was purified by column chromatography on silica gel to give **6e** (50 mg, 51%) and the starting material **6j** (51 mg, 46%).

4.5. General procedure for the synthesis of 7

To pyridinium chloride (60 mmol) that had been preheated at 210 °C for 10 min was added **6** (2.4 mmol); the mixture was maintained at 210 °C for 1 h. The reaction mixture was poured onto ice, and the resulting solution was extracted with diethylether (60 mL×3). The combined organic layer was dried once with brine and then over anhydrous magnesium sulfate. After removal of the solvent by evaporation, the resulting residues were purified by column chromatography on silica gel to afford the corresponding deprotected product.

*4.5.1. 6-(4-Aminophenyl)-2-(4-hydroxyphenyl)carbonylpyrazine (**7b**)*

Yellow solid (205 mg, 78%); mp 197 °C (decomp.). ^{1}H NMR (DMSO-d_6, 400 MHz) δ/ppm 9.16 (s, 1H), 8.62 (s, 1H), 7.86 (d, 2H, J=8.8 Hz), 7.72 (d, 2H, J=8.4 Hz), 6.66 (d, 2H, J=8.8 Hz), 6.44 (d, 2H, J=8.4 Hz), 5.68 (s, 2H). ^{13}C NMR (DMSO-d_6, 100 MHz) δ/ppm 113.9 (×2), 115.4 (×2), 122.0, 126.8, 128.2 (×2), 133.5 (×2), 140.6, 142.2, 149.4, 150.4, 151.3, 162.8, 190.7. IR (KBr) ν_{max}/cm^{-1} 3376, 3333 (νNH), 1651 (νC=O), 1157 (νC–O). FABMS (DTT/TG=1:1) m/z 292 [M+H]$^+$. Anal. Calcd for $C_{17}H_{13}N_3O_2\cdot$0.12AcOEt: C, 69.54; H, 4.66; N, 13.92. Found: C, 69.78; H, 4.58; N, 13.66.

*4.5.2. 2-(4-Hydroxyphenyl)carbonyl-6-phenylpyrazine (**7c**)*

Pale yellow solid (135 mg, 94%); mp 180–181 °C. ^{1}H NMR ($CDCl_3$, 400 MHz) δ/ppm 9.21 (s, 1H), 9.12 (s, 1H), 8.20 (d, 2H, J=8.8 Hz), 8.08 (dd, 2H, J=7.7 and 2.2 Hz), 7.51–7.56 (m, 3H), 6.96 (d, 2H, J=8.8 Hz), 5.90 (s, 1H). ^{13}C NMR ($CDCl_3$, 100 MHz) δ/ppm 115.5 (×2), 127.2 (×2), 128.7, 129.4 (×2), 130.6, 134.1 (×2), 135.6, 143.3, 143.7, 149.9, 150.8, 160.9, 190.7. IR (KBr) ν_{max}/cm^{-1} 3126 (νOH), 1651 (νC=O), 1160 (νC–O). FABMS (DTT/TG=1:2) m/z 277 [M+H]$^+$. Anal. Calcd for $C_{17}H_{12}N_2O_2$: C, 73.90; H, 4.38; N, 10.14. Found: C, 73.90; H, 4.46; N, 9.99.

*4.5.3. 6-(4-Mercaptophenyl)-2-(4-hydroxyphenyl)-carbonylpyrazine (**7d**)*

Orange solid (56.1 mg, 98%); mp 149–150 °C. ^{1}H NMR ($CDCl_3$, 400 MHz) δ/ppm 8.89 (s, 1H), 8.42 (s, 1H), 8.00 (d, 2H, J=8.8 Hz), 7.66 (dd, 2H, J=7.9 and 1.8 Hz), 7.47–7.51 (m, 3H), 6.77 (d, 2H, J=8.8 Hz), 5.36 (s, 1H). ^{13}C NMR (DMSO-d_6, 100 MHz) δ/ppm 115.1 (×2), 126.2, 128.2, 129.8, 130.0 (×2), 133.5 (×2), 135.0 (×2), 140.9, 144.5, 149.6, 155.3, 162.7, 188.6. IR (KBr) ν_{max}/cm^{-1} 3126 (νOH), 1644 (νC=O), 1153 (νC–O). FABMS (DTT/TG=1:2) m/z 309 [M+H]$^+$. Anal. Calcd for $C_{17}H_{12}N_2O_2S$: C, 66.22; H, 3.92; N, 9.08. Found: C, 66.05; H, 4.06; N, 8.68.

*4.5.4. 6-(4-Fuluorophenyl)-2-(4-hydroxyphenyl)carbonylpyrazine (**7f**)*

Yellow-brown solid (92.0 mg, 93%); mp 196–197 °C. ^{1}H NMR (DMSO-d_6, 400 MHz) δ/ppm 10.62 (s, 1H), 9.46 (s, 1H), 8.99 (s, 1H), 8.21 (dd, 2H, J=7.0 and 5.5 Hz), 7.97 (d, 2H, J=8.8 Hz), 7.39 (t, 2H, J=8.8 Hz), 6.91 (d, 2H, J=8.8 Hz). ^{13}C NMR (DMSO-d_6, 100 MHz) δ/ppm 115.4 (×2), 116.1 116.3, 126.6, 129.4, 129.5, 131.8, 133.6 (×2), 143.1, 143.6, 148.6, 149.5, 162.3, 162.9, 190.2. IR (KBr) ν_{max}/cm^{-1} 3291 (νOH), 1644 (νC=O), 1238 (νC–F), 1160 (νC–O). FABMS (DTT/TG=1:1) m/z 295 [M+H]$^+$. Anal. Calcd for $C_{17}H_{11}FN_2O_2\cdot$0.1hexane: C, 69.72; H, 4.02; N, 9.24. Found: C, 69.75; H, 3.88; N, 9.02.

*4.5.5. 6-(4-Biphenylyl)-2-(4-hydroxyphenyl)carbonylpyrazine (**7g**)*

Brown solid (122 mg, 85%); mp 251–252 °C. ^{1}H NMR (DMSO-d_6, 400 MHz) δ/ppm 10.62 (s, 1H), 9.50 (s, 1H), 8.98 (s, 1H), 8.22 (d, 2H, J=8.4 Hz), 7.98 (d, 2H, J=8.8 Hz), 7.84 (d, 2H, J=8.4 Hz), 7.73 (d, 2H, J=7.3 Hz), 7.47 (t, 2H, J=7.3 Hz), 7.38 (t, 1H, J=7.3 Hz), 6.90 (d, 2H, J=8.8 Hz). ^{13}C NMR (DMSO-d_6, 100 MHz) δ/ppm 115.4 (×2), 126.7, 126.8 (×2), 127.4 (×2), 127.6 (×2), 128.1, 129.1 (×2), 133.6 (×2), 134.3, 139.2, 141.9, 143.1, 143.7, 149.2, 149.3, 162.9, 190.3. IR (KBr) ν_{max}/cm^{-1} 3064 (νOH), 1665 (νC=O), 1154 (νC–O). FABMS (DTT/TG=1:1) m/z 353 [M+H]$^+$. Anal. Calcd for $C_{23}H_{16}N_2O_2\cdot$0.2hexane: C, 78.51; H, 4.96; N, 7.57. Found: C, 78.78; H, 4.68; N, 7.50.

*4.5.6. 6-(3-Hydroxyphenyl)-2-(4-hydroxyphenyl)carbonylpyrazine (**7h**)*

Yellow solid (107 mg, 89%); mp 222 °C (decomp.). ^{1}H NMR (DMSO-d_6, 400 MHz) δ/ppm 10.62 (s, 1H), 9.74 (s, 1H), 9.38 (s, 1H), 8.97 (s, 1H), 7.97 (d, 2H, J=8.8 Hz), 7.59 (d, 1H, J=7.7 Hz), 7.52 (s, 1H), 7.34 (t, 1H, J=7.7 Hz), 6.92 (d, 2H, J=8.8 Hz), 6.91 (d, 1H, J=7.7 Hz). ^{13}C NMR (DMSO-d_6, 100 MHz) δ/ppm 113.6, 115.4 (×2), 117.5, 117.8, 126.6, 130.3, 133.6 (×2), 136.6, 143.1, 143.6, 149.5, 149.6, 158.1, 162.9, 190.3. IR (KBr) ν_{max}/cm^{-1} 3388 (νOH), 1638 (νC=O), 1157 (νC–O). FABMS (DTT/TG=1:1) m/z 293 [M+H]$^+$. Anal. Calcd for $C_{17}H_{12}N_2O_3\cdot$0.2AcOEt: C, 69.98; H, 4.42; N, 9.04. Found: C, 69.19; H, 4.20; N, 8.88.

*4.5.7. 6-(3,4-dihydroxyphenyl)-2-(4-hydroxyphenyl)-carbonylpyrazine (**7i**)*

Yellow-brown solid (91.5 mg, 69%); mp 238 °C (decomp.). ^{1}H NMR (DMSO-d_6, 400 MHz) δ/ppm 10.60 (s, 1H), 9.49 (s, 1H), 9.28 (s, 1H), 9.26 (s, 1H), 8.82 (s, 1H), 7.94 (d, 2H, J=8.8 Hz), 7.53 (s, 1H), 7.48 (d, 1H, J=8.1 Hz), 6.90 (d, 2H, J=8.8 Hz), 6.84 (d, 2H, J=8.1 Hz).

^{13}C NMR (DMSO-d_6, 100 MHz) δ/ppm 114.1, 115.4 (×2), 116.1, 118.8, 126.4, 126.7, 133.5 (×2), 141.6, 142.8, 146.0, 148.1, 149.4, 149.9, 162.8, 190.5. IR (KBr) ν_{max}/cm^{-1} 3463, 3159 (νOH), 1640 (νC=O), 1164 (νC–O). FABMS (DTT/TG=1:1) m/z 309 [M+H]$^+$. Anal. Calcd for $C_{17}H_{12}N_2O_4\cdot 0.6H_2O$: C, 63.98; H, 3.98; N, 8.78. Found: C, 63.98; H, 4.13; N, 8.78.

4.6. Synthesis of 6-benzoyl-2-chloropyrazine (8)

A mixture of benzoylchloride (1.15 mL, 9.98 mmol) and tetrakis(triphenylphosphine)palladium (187 mg, 162 μmol) in toluene (300 mL) was stirred at 80 °C for 30 min, under an argon atmosphere. The reaction mixture was cooled once to room temperature, and compound **4** (1.30 g, 3.23 mmol) was added to the mixture. Then, the mixed solution was refluxed for 16 h. After cooling to room temperature, 100 mL of water was added to the reaction mixture and the organic materials were extracted with dichloromethane (100 mL×3). The combined organic layer was dried over anhydrous magnesium sulfate, and the solvent was then removed under reduced pressure. The obtained crude materials were purified by column chromatography on silica gel to afford **8** as a yellow oil (439 mg, 62%). This material was directly used in the next step, without further purification. ^{1}H NMR ($CDCl_3$, 400 MHz) δ/ppm 9.14 (s, 1H), 8.81 (s, 1H), 8.10 (d, 2H, J=7.7 Hz), 7.66 (t, 1H, J=7.7 Hz), 7.54 (t, 2H, J=7.7 Hz).

4.7. Synthesis of 2-benzoyl-6-(4-methoxyphenyl)pyrazine (9)

An analogous reaction of **8** (439 mg, 2.01 mmol) with 4-methoxyphenylboronic acid (370 mg, 2.43 mmol), as described for **5**, yielded **9** as a pale yellow solid (518 mg, 89%); mp 108–109 °C. ^{1}H NMR ($CDCl_3$, 400 MHz) δ/ppm 3.89 (s, 3H), 7.04 (d, 2H, J=8.8 Hz), 7.54 (t, 2H, J=7.3 Hz), 7.66 (t, 1H, J=7.3 Hz), 8.03 (d, 2H, J=8.8 Hz), 8.18 (d, 2H, J=7.3 Hz), 9.09 (s, 1H), 9.17 (s, 1H). ^{13}C NMR (DMSO-d_6, 100 MHz) δ/ppm 55.5, 114.7 (×2), 127.5, 128.6 (×2), 128.6 (×2), 130.8 (×2), 133.7, 135.5, 142.4, 143.7, 148.4, 149.7, 161.3, 192.5. IR (KBr) ν_{max}/cm^{-1} 1664 (νC=O), 1020 (νC–O). FABMS (DTT/TG=1:2) m/z 291 [M+H]$^+$. Anal. Calcd for $C_{18}H_{14}N_2O_2$: C, 74.47; H, 4.86; N, 9.65. Found: C, 74.79; H, 4.94; N, 9.62.

4.8. Synthesis of 2-benzoyl-6-(4-hydroxyphenyl)pyrazine (10)

An analogous reaction of **9** (298 mg, 1.02 mmol) with pyridinium chloride (4.92 g, 42.5 mmol), as described for **7**, yielded **10** as a reddish brown solid (233 mg, 79%); mp 167–168 °C. ^{1}H NMR ($CDCl_3$, 400 MHz) δ/ppm 5.53 (s, 1H), 6.98 (d, 2H, J=8.4 Hz), 7.54 (t, 2H, J=7.7 Hz), 7.66 (t, 1H, J=7.7 Hz), 7.99 (d, 2H, J=8.8 Hz), 8.17 (d, 2H, J=7.7 Hz), 9.09 (s, 1H), 9.16 (s, 1H). ^{13}C NMR (DMSO-d_6, 100 MHz) δ/ppm 116.0 (×2), 125.9, 128.5 (×2), 128.7 (×2), 130.7 (×2), 133.6, 135.5, 142.0, 143.4, 148.3, 150.0, 159.8, 192.5. IR (KBr) ν_{max}/cm^{-1} 3227 (νOH), 1669 (νC=O), 1150 (νC–O). FABMS (DTT/TG=1:2) m/z 277 [M+H]$^+$. Anal. Calcd for $C_{17}H_{12}N_2O_2$: C, 73.90; H, 4.38; N, 10.14. Found: C, 73.99; H, 4.48; N, 10.00.

4.9. Synthesis of 6-(4-acetoxyphenyl)-2-(4-acetoxyphenyl)carbonylpyrazine (11)

An analogous reaction of **1** (111 mg, 379 mmol) with acetic anhydride (0.20 mL, 2.1 mmol), as described for **6f**, yielded **11** as a pale yellow solid (128 mg, 90%); mp 131–132 °C. ^{1}H NMR (DMSO-d_6, 400 MHz) δ/ppm 9.54 (s, 1H), 9.12 (s, 1H), 8.20 (d, 2H, J=8.8 Hz), 8.16 (d, 2H, J=8.8 Hz), 7.38 (d, 2H, J=8.8 Hz), 7.33 (d, 2H, J=8.8 Hz), 2.33 (s, 3H), 2.31 (s, 3H). ^{13}C NMR (DMSO-d_6, 100 MHz) δ/ppm 20.9, 20.9, 122.1 (×2), 122.7 (×2), 128.4 (×2), 132.5 (×2), 132.8, 132.8, 143.4, 144.3, 148.4, 149.0, 152.2, 154.5, 168.9, 169.1, 191.1. IR (KBr) ν_{max}/cm^{-1} 1755, 1712 (νC=O), 1177, 1143 (νC–O). FABMS (DTT/TG=1:2) m/z 377 [M+H]$^+$. Anal. Calcd for $C_{21}H_{16}N_2O_5$: C, 67.02; H, 4.28; N, 7.44. Found: C, 67.03; H, 4.34; N, 7.36.

4.10. Synthesis of (4-methoxyphenyl)pyrazine (12)

A mixture of 2-chloropyrazine (54.0 mg, 0.47 mmol), 4-methoxyphenylboronic acid (82.1 mg, 0.54 mmol), and palladium(II) acetate (9.9 mg, 44 μmol) in dimethoxyethane (1 mL) was stirred at 80 °C for 35 min. To the mixture was added 0.7 mL of 2 M K_2CO_3, and the mixed solution was refluxed for 1.5 h. After cooling to room temperature, water (20 mL) was added to the reaction mixture; the organic materials were extracted with ethyl acetate (20 mL×3). The combined organic layer was dried over anhydrous magnesium sulfate, and the solvent was then evaporated. The resulting residues were purified by column chromatography on silica gel to afford **12** as a colorless powder (82.1 mg, 94%); mp 88–89 °C. ^{1}H NMR ($CDCl_3$, 400 MHz) δ/ppm 8.99 (d, 1H, J=1.5 Hz), 8.59 (dd, 1H, J=2.6 and 1.5 Hz), 8.45 (d, 1H, J=2.6 Hz), 7.99 (d, 2H, J=8.8 Hz), 7.04 (d, 2H, J=8.8 Hz), 3.87 (s, 3H). ^{13}C NMR (DMSO-d_6, 100 MHz) δ/ppm 55.3, 114.5(×2), 128.2, 128.2(×2), 141.4, 142.5, 144.1, 151.3, 160.8. IR (KBr) ν_{max}/cm^{-1} 1251, 1036 (νC–O). FABMS (DTT/TG=1:2) m/z 187 [M+H]$^+$. Anal. Calcd for $C_{11}H_{10}N_2O$: C, 70.95; H, 5.41; N, 15.04. Found: C, 71.01; H, 5.41; N, 14.99.

4.11. Synthesis of (4-hydroxyphenyl)pyrazine (13)

An analogous reaction of **12** (49.3 mg, 0.265 mmol) with pyridinium chloride (2.80 g, 24.2 mmol), as described for **7**, yielded an orange solid (40.0 mg, 88%); mp 214–215 °C. ^{1}H NMR (DMSO-d_6, 400 MHz) δ/ppm 9.14 (d, 1H, J=1.5 Hz), 8.62 (dd, 1H, J=2.2 and 1.5 Hz), 8.49 (d, 1H, J=2.2 Hz), 8.00 (d, 2H, J=8.8 Hz), 6.90 (d, 2H, J=8.8 Hz). ^{13}C NMR (DMSO-d_6, 100 MHz) δ/ppm 115.9 (×2), 126.7, 128.2 (×2), 141.2, 142.1, 144.0, 151.6, 159.3. IR (KBr) ν_{max}/cm^{-1} 3057, 3018 (νOH), 1281 (νC–O). FABMS (DTT/TG=1:2) m/z 173 [M+H]$^+$. Anal. Calcd for $C_{10}H_8N_2O$: C, 69.76; H, 4.68; N, 16.27. Found: C, 69.99; H, 4.77; N, 16.16.

4.12. Enzyme activity assay

Enzyme activity was measured by monitoring the decay in absorbance at 340 nm, which accompanies the oxidation of NADPH catalyzed by h-ALR2. The reaction mixture contained 0.2 M phosphate buffer (pH 6.2), 0.15 mM NADPH, 10 mM D,L-glyceraldehyde, and 3.6 mU/mL h-ALR2, in a total volume of 1.0 mL. All the above reagents, except D,L-glyceraldehyde, were incubated at 25 °C for 1 min. The reaction was initiated by the addition of D,L-glyceraldehyde, and it was monitored spectrophotometrically for 5 min at the same temperature. Inhibitory activity was tested in the above assay conditions by including the inhibitors dissolved in dimethyl sulfoxide (DMSO) at desired concentrations in the reaction mixture. The final concentration of DMSO in the reaction mixture was kept at a constant concentration of 0.3%. Reference blank assays, lacking either the substrate or enzyme, were routinely included; the rates were subtracted from the reaction rates, to correct for the non-enzymatic oxidation of NADPH. IC_{50} values, which express the inhibitor concentrations that produce the 50% inhibition on the oxidation of NADPH calatyzed by h-ALR2, were calculated using a log linear regression analysis of the log dose–inhibition plots. Each plot was provided, using at least three concentrations of inhibitor with two replicates at each concentration.

4.13. Enzyme kinetics

Kinetic parameters were determined in the same manner as the enzyme activity assay, except the substrate concentrations were changed. Each initial velocity value was determined in triplicate,

over at least five different substrate concentrations. The Michaelis constant (K_m) and the maximum velocity (V_{max}) of the enzyme with respect to the substrate were determined from the double reciprocal plot of initial velocity versus substrate concentration in the absence of inhibitors. In the presence of mixed-type inhibitors, the initial velocity (V) changed as follows:[31]

$$V = V_{max}[S]/\{K_m(1+[I]/K_i)+[S](1+[I]/K_i')\},$$

where [S] is the substrate concentration, [I] is the inhibitor concentration, and K_i and K_i' are the dissociation constants of the enzyme–inhibitor complex and the enzyme–substrate–inhibitor ternary complex, respectively. According to this equation, the apparent K_m ($K_{m,app}$) and V_{max} ($V_{max,app}$) in the presence of inhibitors are expressed as follows:

$$K_{m,app} = (\alpha/\alpha')K_m$$

$$V_{max,app} = V_{max}/\alpha',$$

where α and α' donate the factors $1+([I]/K_i)$ and $1+([I]/K_i')$, respectively.[23,25] Thus, kinetic constants in the presence of inhibitors were determined by applying the above equations to the double reciprocal plots. Data are expressed as mean±standard deviation for repeated runs. A statistical analysis was performed using a Student's t-test at the 5% significance level of difference ($p<0.05$).

Acknowledgements

This research was supported by the Special Grant for Collaborations Across the Colleges at Toho University.

Supplementary data

Supplementary data associated with this article can be found in the online version, at doi:10.1016/j.tet.2009.01.020.

References and notes

1. Kador, P. F.; Kinoshita, J. H.; Sharpless, N. E. *J. Med. Chem.* **1985**, *28*, 841.
2. Dvornik, D. *Aldose Reductase Inhibition: An Approach to the Prevention of Diabetic Complications*; McGraw-Hill: New York, NY, 1987.
3. Nishimura, C. *Pharmacol. Rev.* **1998**, *50*, 21.
4. Costantino, L.; Rastelli, G.; Paola, V.; Cignarella, G.; Barlocco, D. *Med. Res. Rev.* **1999**, *19*, 3.
5. Brownlee, M. *Nature* **2001**, *414*, 813.
6. Lorenzi, M. *Exp. Diabetes Res.* **2007**, 2007:61038.
7. Pfeifer, M. A.; Schumer, M. P. *Diabetes* **1995**, *44*, 1355.
8. Costantino, L.; Rastelli, G.; Cignarella, G.; Vianello, G.; Barlocco, D. *Expert Opin. Ther. Pat.* **1997**, *7*, 843.
9. Costantino, L.; Rastelli, G.; Gamberini, M. C.; Barlocco, D. *Expert Opin. Ther. Pat.* **2000**, *10*, 1245.
10. Miyamoto, S. *Chem-Bio Informatics J.* **2002**, *2*, 74.
11. Durán, R.; Zubía, E.; Ortega, M.; Naranjo, S.; Salva, J. *Tetrahedron* **1999**, *55*, 13225.
12. Manzanaro, S.; Salvá, J.; De la Fuente, J. A. *J. Nat. Prod.* **2006**, *69*, 1485.
13. Kador, P.; Lee, Y. S.; Rodriguez, L.; Sato, S.; Bartoszko-Malik, A.; Abdel-Ghany, Y. S.; Miller, D. D. *Bioorg. Med. Chem.* **1995**, *3*, 1313.
14. (a) Ishii, A.; Kotani, T.; Nagaki, Y.; Shibayama, Y.; Toyomaki, Y.; Okukado, N.; Ienaga, K.; Okamoto, K. *J. Med. Chem.* **1996**, *39*, 1924; (b) Negoro, T.; Murata, M.; Ueda, S.; Fujitani, B.; Ono, Y.; Kuromiya, A.; Komiya, M.; Suzuki, K.; Matsumoto, J. *J. Med. Chem.* **1998**, *41*, 4118; (c) Oka, M.; Matsumoto, Y.; Sugiyama, S.; Tsuruta, N.; Matsushima, M. *J. Med. Chem.* **2000**, *43*, 2479; (d) Bruno, G,; Costantino, L.; Curinga, C.; Maccari, R.; Monforte, F.; Nicolò, F.; Ottanà, R.; Vigorita, M. C. *Bioorg. Med. Chem.* **2002**, *10*, 1077; (e) Maccari, R.; Ottanà, R.; Curinga, C.; Vigorita, M. G.; Rakowitz, D.; Steindl, T.; Langer, T. *Bioorg. Med. Chem.* **2005**, *13*, 2809.
15. Shimomura, O.; Johnson, F. H. *Tetrahedron Lett.* **1973**, *14*, 2963.
16. Goto, T.; Iio, H.; Inoue, S.; Kakoi, H. *Tetrahedron Lett.* **1974**, 2321.
17. (a) Saito, R.; Hirano, T.; Niwa, H.; Ohashi, M. *J. Chem. Soc., Perkin Trans. 2* **1997**, 1171; (b) Saito, R.; Hirano, T.; Niwa, H.; Ohashi, M. *Chem. Lett.* **1998**, *27*, 95; (c) Saito, R.; Inoue, C.; Katoh, A. *Heterocycles* **2004**, *63*, 759; (d) Saito, R.; Machida, S.; Suzuki, S.; Katoh, A. *Heterocycles* **2008**, *65*, 531.
18. Buron, F.; Plé, N.; Turck, A.; Queguiner, G. *J. Org. Chem.* **2005**, *70*, 2616.
19. Nishimura, C.; Yamaoka, T.; Mizutani, M.; Yamashita, K.; Akera, T.; Tanimoto, T. *Biochim. Blophys. Acta* **1991**, *1078*, 171.
20. Del Corso, A.; Costantino, L.; Rastelli, G.; Buono, F.; Mura, U. *Exp. Eye Res.* **2000**, *71*, 515.
21. Terashima, H.; Hama, K.; Yamamoto, R.; Tsuboshima, M.; Kikkawa, R.; Hatanaka, I.; Shigeta, Y. *J. Pharmacol. Exp. Ther.* **1984**, *229*, 226.
22. Kato, K.; Nakayama, K.; Mizota, M.; Miwa, I.; Okuda, J. *Chem. Pharm. Bull.* **1991**, *39*, 1540.
23. Dixon, M.; Webb, E. C. *Enzymes*, 3rd ed.; Longman: London, 1979.
24. Barrett, A. J.; Salvesen, G.; Dingle, J. T. *Proteinase inhibitors*; Elsevier: Amsterdam, 1990.
25. Copeland, R. A. *Enzymes*, 2nd ed.; Wiley-VCH: New York, NY, 2000.
26. Peterson, M. J.; Sarges, S.; Aldinger, C. E.; MacDonald, D. P. *Metabolism* **1979**, *28*, 456.
27. Wilson, D. K.; Tarle, I.; Petrash, M.; Quiocho, F. A. *Proc. Natl. Acad. Sci. U.S.A.* **1993**, *90*, 9847.
28. Kurono, M.; Fujiwara, I.; Yoshida, K. *Biochemistry* **2001**, *40*, 8216.
29. Ward, W. H. J.; Sennitt, C. M.; Ross, H.; Dingle, A.; Timms, D.; Mirrlees, D.; Tuffin, D. P. *Biochem. Pharmacol.* **1990**, *39*, 337.
30. Kishi, Y.; Tanino, H.; Goto, T. *Tetrahedron Lett.* **1972**, *13*, 2747.
31. Cook, P. N.; Ward, W. H. J.; Petrash, J. M.; Mirrlees, D. J.; Sennitt, C. M.; Carey, F.; Preston, J.; Brittain, D. R.; Tuffin, D. P.; Howe, R. *Biochem. Pharmacol.* **1995**, *49*, 1043.